Title: Tick-borne flaviviruses alter membrane structure and replicate in dendrites of primary mouse neuronal cultures

Running title: Replication mechanism of TBEV in mouse primary neuron

Contents category: Standard paper

Authors: Minato Hirano 1), Kentaro Yoshii 1), Mizuki Sakai 1), Rie Hasebe 2), Osamu Ichii 3), Hiroaki Kariwa 1)

1) Laboratory of Public Health, Graduate School of Veterinary Medicine, Hokkaido University, Sapporo, Japan

2) Laboratory of Veterinary Hygiene, Graduate School of Veterinary Medicine, Hokkaido University, Sapporo, Japan

3) Laboratory of Anatomy, Graduate School of Veterinary Medicine, Hokkaido University, Sapporo, Japan

Corresponding author: Kentaro Yoshii,

Postal address: Laboratory of Public Health, Graduate School of Veterinary Medicine, Hokkaido University, kita-18 nishi-9, kita-ku, Sapporo, Hokkaido 060-0818, Japan

Tel/fax: +81-11-706-5213

E-mail: kyoshii@vetmed.hokudai.ac.jp

Word count: Summary (224 words), Main text (5350 words)

Summary

Neurological diseases caused by encephalitic flaviviruses are severe and associated with high level of mortality. However, detailed mechanisms of viral replication in the brain and features of viral pathogenesis remain poorly understood. We carried out the comparative analysis of replication of neurotropic flaviviruses, West Nile virus, Japanese encephalitis virus, and tick-borne encephalitis virus (TBEV), in primary cultures of mouse brain neurons. All flaviviruses multiplied well in the primary neuronal cultures from hippocampus, cerebral cortex, or cerebellum. Distribution of viral-specific antigen in the neuron varied; TBEV infection induced the accumulations of viral antigen in the neuronal dendrites to greater extent than did infection with other viruses. Viral structural, non-structural proteins, and double-stranded RNA were detected in the regions of which viral antigens accumulated in dendrites after TBEV replication. Replication of TBEV replicon after the infection of TBEV virus-like particles also induced the antigen accumulation, indicating that accumulated viral antigens were the results of the viral RNA replication. Further, electron microscopic observation confirmed that TBEV replication induced the characteristic ultrastructural membrane alterations in the neurites; newly formed laminal membrane structure containing virion-like structures. This is the first report describing viral replication in and ultrastructural alterations of the neuronal dendrites, possibly causing the neuronal dysfunction. These findings encourage further study to understand the molecular mechanisms of viral replication in brains and the pathogenicity of neurotropic flaviviruses.

Introduction

Flavivirus is a genus in the family *Flaviviridae*, and consists of positive-polarity single-strand RNA viruses with lipid envelopes (Gould & Solomon, 2008; Lindenbach, 2007; Schmaljohn & McClain, 1996). The flavivirus genome encodes one poly polyprotein, which is cleaved into three structural proteins, the core, premembrane, and envelope (E) proteins, and seven non-structural (NS) proteins within a single long open reading frame (Chambers *et al.*, 1990). *Flavivirus* contains over 70 members, many of which are arthropod-borne human pathogens (Lindenbach, 2007; Mackenzie *et al.*, 2004; Mackenzie & Williams, 2009; Schmaljohn & McClain, 1996). Recently, many outbreaks have been reported, and flaviviruses are attracting global attention as emerging or re-emerging infectious diseases (Balogh *et al.*, 2010; Chung *et al.*, 2013; Danis *et al.*, 2011; McMichael *et al.*, 2006; Morse, 1995; Vong *et al.*, 2010). Flaviviruses are divided into four distinct evolutionary lineages: mosquito-borne, tick-borne, no-known vector, and insect-only flaviviruses (Billoir *et al.*, 2000; Cook *et al.*, 2012; Crabtree *et al.*, 2003; Kuno *et al.*, 1998). Mosquitoes of *Aedes* and *Culex* families are the major vector of mosquito-borne flaviviruses, including yellow fever virus, dengue virus, West Nile virus (WNV), and Japanese encephalitis virus (JEV) (Gould & Solomon, 2008). *Ixodidae* ticks carry tick-borne flaviviruses, including tick-borne encephalitis virus (TBEV) and Langat virus (LGTV) (Lindquist & Vapalahti, 2008).

Flavivirus infection of human causes various manifestations, hemorrhagic disease, encephalitis, biphasic fever, flaccid paralysis, and jaundice (Gould & Solomon, 2008). Encephalitis, a neurological manifestation of disease, is particularly problematic. This condition is associated with high-level mortality and severe sequelae. All of WNV, JEV, and TBEV are principal neurotropic flaviviruses causing encephalitic diseases in humans. Common symptoms are headache, vomiting, ataxia, and paralysis. Differences in neurologic symptoms have been reported in the infection of

each virus. JEV infection triggers acute spasm and development of a dull pathognomonic Parkinsonian syndrome (Ooi *et al.*, 2008; Solomon *et al.*, 1998). Cognitive function is compromised upon several cases of TBEV infection; patients develop photophobia, irritability, and sleeping disorders (Czupryna *et al.*, 2011; Kaiser, 1999; Mickiene *et al.*, 2002). WNV infection triggers development of systemic symptoms generally, but neurologic manifestations are rare (Anastasiadou *et al.*, 2013; Sejvar *et al.*, 2003). On histopathological examinations, all these viruses mentioned above induce typical nonsuppurative encephalitis, including necrosis of neurons (associated with shrunken perikarya), perivascular and vascular infiltration of mononuclear cells, and neuronophagia. The distribution of viral antigens in the cerebellum differs, but viral antigens are seen in several brain regions among all viruses, including the brainstem, the cerebral cortex, the caudate putamen, and the cervical spinal cord (Hayasaka *et al.*, 2009; Kimura *et al.*, 2010). However, it remains unclear how viral replication and pathogenicity contributes to the neurologic manifestations.

Primary culture has been developed for maintaining brain cells (Banker & Cowan, 1977), and such cultures can be used to investigate detailed intracellular activities of neurons (Ishihara *et al.*, 2009; Okabe, 2013; Wang *et al.*, 2009). This approach has been used to explore not only physiological functions, but also neuronal response affected by virus invasion, including lyssavirus, herpesvirus, and flaviviruses (Lewis & Lentz, 1998) (Perkins *et al.*, 2002) (Chen *et al.*, 2011). Primary cultured neurons could provide detailed information about flavivirus replication in neurons.

In the present study, we used primary neuronal cultures to explore replicative and neuropathogenic features of encephalitic flaviviruses. We revealed that the replicative properties of mosquito and tick-borne flaviviruses differed significantly.

Results

72

73 **Replication of neurotropic flaviviruses in primary neuronal cultures**

74 Prior to experiments using infectious viruses, cell components of primary cultured brain cells were
75 examined. Primary neuronal cultures were prepared from hippocampi, cerebral cortexes, and
76 cerebella, and stained for a neuronal marker (microtubule-associated protein 2: MAP2, green),
77 astroglial marker (Glial fibrillary acidic protein: GFAP, red), and DAPI (blue), via indirect
78 immuofluorescent assay (IFA). Fig. S1 shows that the primary cultures contained principally
79 neurons (70−80%) and astroglial cells (20%), and lacked microglial cells (data not shown).

80

81 To compare growth kinetics of encephalitic flaviviruses, primary cultures from each region were
82 infected with TBEV, WNV, or JEV at an multiplicity of infection (MOI) of 0.1, and viral titers in the
83 culture supernatant were measured at various time points, the experiments were repeated four times.
84 Fig. 1a and 1b show that viral titers peaked at 48 h.p.i., and the titers did not differ among studied
85 primary cultures. The viral titer of TBEV at 48 h.p.i. was slightly higher than that attained by the
86 other viruses, but the difference was not statistically significant. Viral growth kinetics was similar
87 all studied primary cultures. Thus, cerebral cortex cells were used in all subsequent experiments. No
88 obvious morphological change evident upon light microscopy, apart from slight dendritic
89 degeneration in TBEV-infected neurons (Fig. 1c).

90

91 **Distribution of viral antigen in primary neuronal cultures**

92 The distribution of viral antigens in primary neuronal cultures was examined via IFA. At 48 h.p.i.,
93 infected cells stained with MAP2 (a marker of neuronal cell body and dendrites, green),
94 virus-specific antibodies (red), and DAPI (blue). Fig. 2a shows that the cell body distribution of
95 viral antigens was similar in neurons infected with each virus studied. However, dendritic
96 distributions were different in infected neurons. Viral antigens were sparsely distributed in dendrites

of cells infected with WNV or JEV (Fig. 2a vii, viii, xii, and xiii). On the other hand, elliptical antigen accumulations were evident in dendrites infected with TBEV (Fig. 2a ii and iii, white arrows). This form of antigen-accumulation was also evident in neurons infected with the tick-borne flaviviruses, TBEV, Omsk hemorrhagic fever virus (OHFV), and LGTV (Fig. S2).

Detailed images of accumulated viral antigens are shown in Fig. 2b. Antigen accumulations varied in diameter, being 5−10 μm on the major and 3−5 μm on the minor axis (Fig. 2b iii, iv, vi, and vii). Viral antigens were surrounded by MAP2 in structures that appeared to be swollen (Fig. 2b iv and vii). In some large swellings, an unstained (hollow) region was evident within the accumulation of viral antigen (Fig. 2b ii-iv).

Changes over time in viral antigen distribution are shown in Fig. 3. In the early stages of TBEV infection, viral antigens were detected in the cell body principally, thus minimally the dendrites (Fig. 3a i and ii). From 48−72 h.p.i., viral antigen accumulated in the dendrites (Fig. 3a iii and iv, white arrows). However, viral antigen in WNV or JEV infected cells was located principally in the cell body (thus minimally in the dendrites) at all timepoints examined (Fig. 3a v-viii, and ix-xii). WNV antigen accumulated in dendrites of several neurons by 72 h.p.i. (Fig. 3a viii, white arrows), but such accumulations were fewer compared with in neurons infected with TBEV (Fig. 3b).

In a previous study, TBEV infection triggered microtubule re-arrangement in neuroblastoma cells (Ruzek *et al.*, 2009), possibly associated with the viral antigen accumulations in dendrites. As shown in Fig. 4, neurons mock-infected (Fig. 4a−d) or infected with TBEV (Fig. 4e−ab) were co-stained with the anti-TBEV and anti-MAP2 (Fig. 4a and e-j), anti-β3-tublin (Fig. 4b and k-p), anti-calreticulin (Fig. 4c and q-v), or anti-synaptophysin (Fig. 4d and w-ab) antibodies. However, no obvious change in microtubules distribution was evident in infected primary neuronal cultures

(Fig. 4k−p). Accumulated viral antigens in TBEV infected cells were localized with MAP2 (Fig. 4h−j), β3-tublin (Fig. 4n−p), or calreticulin, which is distributed in endoplasmic reticulum (ER) membrane (Fig. 4t-v), but not with synaptophysin, a marker of synaptic vesicles (Fig. 4z−ab). Thus, the viral antigens accumulated in the ER of the dendrites, but it was not directly associated with rearrangement of microtubules and synaptic vesicles.

Effect of perturbation of microtubule on viral antigen distribution

Addition of nocodazole (which disrupts microtubules) induced dendrite loss (Fig. 5a−c), and TBEV or WNV antigens were present in the neural cell body only (Fig. 5d−f, and g−i). Thus, the viral antigen accumulations were affected by microtubule.

Viral constituent of the protein accumulations in dendrites

Viral constituents in accumulations were investigated. Staining of TBEV-infected neurons with specific antibodies detecting structural (E) and non-structural (NS3) proteins showed that both proteins were present in the antigen accumulations (Fig. 6a i, iii, iv, and vi, white arrows). In addition, double stranded RNA: dsRNA (reflecting viral genome replication) was also present (Fig. 6b vi and vii). These results suggest that viral genome replication occurred in the regions of viral protein accumulations in dendrites.

To investigate the viral components required for the formation of the accumulated viral antigens, we next infected primary cultures with virus-like particles (VLPs) of TBEV ("single-round" infectious particles containing replicon RNA as a genome) (Gehrke *et al.*, 2003; Khromykh *et al.*, 1998; Molenkamp *et al.*, 2003; Reynard *et al.*, 2011; Yoshii *et al.*, 2008). The replicon RNA lacks the most of the cording region for viral structural proteins. The VLPs can enter cells, and replicate within, but cannot produce a progeny virus. Fig. 6c shows that viral antigen also accumulated in

147 dendrites after infection of the TBEV-VLPs (Fig. 6c i−iv, white arrows). Thus, viral protein
148 accumulations did not require expression of viral structural proteins.
149
150 **The ultrastructure of flavivirus infected primary cultured neuron.**
151 To observe the membrane structure of infected neurites, infected primary neuronal cultures were
152 examined by transmission electron microscopy (TEM) (Fig. 7). Mock infected neurons had large
153 nuclei, and ER, mitochondria, and Golgi apparatus were readily observed (Fig. 7a−c). However,
154 virus-infected neurons exhibited cytoplasmic condensation with granular structures, and reactive
155 lyososomes were evident (Fig. 7d). Apoptotic cells (identified by nuclear distortion or the presence
156 of apoptotic bodies) were rare. The spherical virion-like structures coated with lipid bilayer were
157 observed in infected neurons (Fig. 7e). The cell bodies of neurons infected with TBEV or WNV
158 were similar in appearance. Organized microtubules were observed in neurites of mock-infected
159 neurons (Fig. 7f). After infection of WNV, degenerated membrane and granular structures appeared
160 in neurites (Fig. 7g). In contrast, TBEV infection caused neurite swelling and appearance of
161 elliptical structures (Fig. 7h and i). These structures were surrounded by laminal membranes and
162 adjacent to microtubules (Fig. 7i). Virion-like structures coated with lipid bilayers were observed
163 both inside and outside of these structures (Fig. 7j-l). Infection with either WNV or TBEV
164 infection triggered neuronal cytoplasmic condensation. TBEV infection caused a characteristic
165 ultrastructural change of membrane in the neurites: a laminal membrane structure (LMS) besides
166 the microtubules. WNV infection was not associated with LMS formation.
167
168 ## Discussion
169
170 Despite the importance of neuro-pathogenicity of TBEV, the detailed feature of the replication
171 mechanism in the neural cells is still unknown. We used primary cultures of brain cells to

172 comparatively examine the replication of several flaviviruses. Viral antigen distribution in infected
173 primary neuronal cultures differed when such cells were infected with the mosquito and tick-borne
174 neurotropic flaviviruses. IFA and TEM studies revealed that dendritic replication of tick-borne
175 flaviviruses caused abnormal swelling of neurites and development of a specific structure, LMS.
176
177 Each studied flavivirus multiplied effectively in primary neuronal cultures from several brain
178 regions, indicating that use of such cells is appropriate when investigating flavivirus infection. But,
179 the flaviviruses showed similar growth kinetics in primary cultures from several brain regions.
180 Neurotropic flaviviruses have been reported to exhibit differences in distribution and multiplication
181 among the various parts of the brain. WNV antigens were less detected in granule cell neurons of
182 the cerebellum compared with other neuronal populations (Omalu *et al.*, 2003; Xiao *et al.*, 2001). In
183 contrast, JEV replicated well in granule cell neurons (Desai *et al.*, 1995; German *et al.*, 2006), and
184 TBEV replicated throughout the cerebellum, including granule cells (Gelpi *et al.*, 2005; Hayasaka *et*
185 *al.*, 2009). Two possible reasons may be suggested to explain the difference in the *in vivo* and *in*
186 *vitro* results. First, lack of glial cell maturation may influence viral replication. Mammalian neurons
187 interact with glial cells soon after birth; the neurons mature and become myelinated (Baumann &
188 Pham-Dinh, 2001). Some reports have emphasized that the presence of glial cells is important for
189 effective flavivirus replication in the brain (Chen *et al.*, 2010; Hussmann *et al.*, 2013). It is possible
190 that primary viral replication in glial cells is essential if the viruses are subsequently to spread
191 efficiently through the brain. Second, incomplete maturation of the innate immune response of
192 neurons may affect the susceptibility of such cells to flavivirus infection. The granule cells of the
193 cerebellum have been reported that to mount an effective innate immune response against viral
194 infection (Cho *et al.*, 2013). The primary cell cultures used in the present study were devoid of glial
195 cells (except astroglias), and embryonic neurons may lack a well-developed innate immune system.
196 Thus, the susceptibility of primary embryonic neuronal cultures to viral infection may differ from

197 that of adult brains *in vivo*. Interferon treatment of primary neuronal cultures may render viral
198 replication patterns similar to those observed *in vivo*.
199
200 Infection with tick-borne flaviviruses was associated with accumulations of viral antigens in the
201 dendrites of infected neurons, but this was not true of mosquito-borne flavivruses. The
202 accumulations contained structural proteins, non-structural proteins, and dsRNA. Accumulations
203 were also evident upon the replication of replicon RNA after infection with VLPs of TBEV.
204 Flaviviruses replicate at ER membranes, and buds into the ER lumen (Lindenbach, 2007). Dendrites
205 are known to contain free ribosomes and express satellite secretory pathways to secure synaptic
206 plasticity (Martone *et al.*, 1993; McCarthy & Milner, 2003; Ori-McKenney *et al.*, 2012; Pierce *et al.*,
207 2001; Ramirez & Couve, 2011). Together, the data suggest that tick-borne flaviviral replication in
208 dendrites induced viral protein accumulation. Infection with rabies virus, influenza virus, and other
209 viruses similarly accumulated viral antigens in the dendrites previously (Li *et al.*, 2005; Matsuda *et*
210 *al.*, 2005). Such accumulation has been considered to reflect inhibition of viral protein
211 transportation in dendrites in which cytoskeleton has been disrupted. However, we found that the
212 mechanism of antigen accumulations during TBEV infection were quite different. This is the first
213 report to show the tick-borne flaviviral replication in dendrites.
214
215 TBEV infection caused a characteristic ultrastructural change in neurite membranes of infected
216 neuron. An LMS developed, lying parallel to microtubules, and virion-like structures were observed
217 both inside and outside of this structure. The co-localization of the viral antigen and ER marker
218 indicated the LMS were derived from ER-membrane. LMS-like membranes were previously
219 observed in glioblastoma cells infected with TBEV (Ruzek *et al.*, 2009). Flavivirus infection
220 induces typical alterations in ER membranes. The membranes assume vesicle packets (VPs) and
221 convoluted membranes (CM) (Mackenzie, 2005), forming a platform on which viral genome

222 replication and virion assembly proceed (Uchil & Satchidanandam, 2003; Welsch *et al.*, 2009). It is
223 possible that LMS is formed via ER-derived membrane reconstitution triggered by the viral
224 replication, and serves as the scaffold for dendritic viral replication and virion assembly. The
225 unstained hollow regions evident when the accumulations of viral proteins were examined by IFA
226 may be attributable to the fact that degenerated membranes are poorly permeable to antibodies.
227
228 A proposed model of LMS formation is shown in Fig. 8. Viral proteins are synthesized in dendrites
229 (Fig. 8a). Membrane structures are reconstituted to form the LMS after such synthesis (Fig. 8b), and
230 the LMS becomes multilayered and grows to compress the microtubules (Fig. 8c).
231
232 Time-course experiments revealed that viral proteins were synthesized principally in the neuronal
233 cell bodies during the early stages of infection, becoming distributed in dendrites only later. Thus,
234 TBEV genomic RNA (with or without viral proteins) was transported principally from cell bodies to
235 dendrites. Viral genomic RNA bound to membrane-associated replication complex (formed by viral
236 non-structural proteins) may be transported along dendritic membrane. Another important transport
237 mechanism involves formation of RNA granules. Recently, mRNA transportation to the dendrites,
238 and local translational control therein, have been described in neuron (Kiebler & DesGroseillers,
239 2000; Kohrmann *et al.*, 1999; Muramatsu *et al.*, 1998; Sinnamon & Czaplinski, 2011). Specific
240 mRNAs form RNA granules containing several different RNA binding proteins are transported
241 along microtubules to dendrites in a kinesin-dependent manner (Bramham & Wells, 2007; Kanai *et*
242 *al.*, 2004). It is possible that viral genomic RNAs may hijack or mimic this transport mechanism.
243 Microtubule-dependent formation of viral antigen accumulations in dendrites may support this
244 hypothesis.
245
246 All tick-borne flaviviruses used in the present study, Far Eastern and European subtype of TBEV,

247 OHFV, and LGTV, accumulated viral antigens in dendrites. However, WNV and JEV formed
248 smaller accumulations. Some previous studies used the primary brain cultures to investigate
249 replication of mosquito-borne flaviviruses, but no mention was made of the viral antigen
250 accumulation in dendrites (Chen *et al.*, 2011; Diniz *et al.*, 2006). Tick-borne flaviviruses share the
251 characteristics in viral antigen accumulation in dendrites.
252
253 Alteration in membrane structure and accumulation of viral proteins in dendrites may cause the
254 neuronal dysfunction and degeneration *in vivo*. LMS formation and viral protein accumulation
255 induced ultrastructural changes in neurites, including compression of the microtubules, the
256 obstruction of trafficking pathways, and reconstitution of membrane structure. Such changes may
257 affect synaptic function and induce neurite degeneration leading to development of neurological
258 disease. Synaptic connections are dynamically regulated via intracellular trafficking pathways,
259 protein modifications, and local protein synthesis in the dendrites (Bagni & Greenough, 2005;
260 Kiebler & DesGroseillers, 2000; McCarthy & Milner, 2003; Steward & Schuman, 2003). Such
261 connections play important roles in the brain, being in recognition, memory, and behavioral
262 regulation. Dendritic degeneration occurs in some diseases associated with loss of cognitive
263 function, including Alzheimer's disease, fragile-X syndrome, and Rett syndrome (Calon *et al.*,
264 2004; Comery *et al.*, 1997; Maezawa & Jin, 2010). Especially, fragile-X syndrome is caused by
265 disruption of local protein synthesis in dendrites, and triggers hyperactivity and greater response to
266 low-intensity auditory stimuli in mouse model (Bagni & Greenough, 2005; Consortium, 1994). As
267 observed in fragile-X syndrome, the abnormal membrane alterations in dendrites by TBEV infection
268 might cause disruption of local protein synthesis in dendrites, resulting in cognitive compromise
269 observed in TBEV patients. In addition, viral protein accumulations in dendrites may affect neural
270 function via the interaction of such proteins with host factors. In a previous study, TBEV replication
271 arrested the neurite outgrowth in a cell line derived from a phenochromocytoma of the rat adrenal

medulla. Such arrest was caused by interaction between TBEV NS5 protein and host proteins-Rac1 and Scribble (Wigerius *et al.*, 2010). The latter proteins are involved in maintaining cell polarity, regulation of synaptic plasticity, and synaptic vesicle dynamics (Roche *et al.*, 2002). It is possible that the accumulated viral proteins affect the distribution and functionality of host proteins with which the viral proteins interact, in turn causing neural dysfunction and cell-degeneration.

In conclusion, we have shown that mosquito and tick-borne flaviviruses replicated differently in primary neuronal cultures. Tick-borne flaviviruses induced ultrastructural membrane alterations and replication thereof was associated with accumulation of viral proteins in dendrites; this was not true of WNV or JEV. We have also shown, for the first time that tick-borne flaviviruses replicate in the neural dendrites. These findings encourage further study to understand the molecular mechanism of viral replication in brains and the pathogenicity of neurotropic flaviviruses, and also promote study to learn how to prevent and cure viral infections.

Methods

Cell culture

Baby hamster kidney-21 (BHK-21) cells were grown at 37°C in minimum essential medium (Life Technologies Co., Carlsbad, CA) supplemented with 8% (v/v) fetal bovine serum and penicillin/streptomycin. Human embryonic kidney 293T cells were cultured at 37°C in Dulbecco's modified Eagle's medium (Life Technologies), containing 10% (v/v) fetal bovine serum and penicillin/streptomycin.

Pregnant Slc: ICR mice were purchased from Japan SLC Inc. (Shizuoka, Japan), and hippocampal, cerebral cortical, and cerebellar neuronal cultures were established from brain cells of these animals.

297 Neurons for primary culture were prepared from embryonic day 17−18 mouse embryos as described
298 previously (Biederer & Scheiffele, 2007; Viesselmann *et al.*, 2011). Briefly, the hippocampus,
299 cerebral cortex, and cerebellum were dissected from embryonic brains into dissection medium:
300 HBSS (Life Technologies) supplemented with 10 mM HEPES (Life Technologies) and 1 mM
301 sodium pyruvate (Life Technologies). Tissues were treated with 0.0125% (w/v) trypsin (Becton
302 Dickinson, Co., Franklin Lakes, NJ) for 5 min at 37°C, and gently dissociated via trituration in
303 neuronal medium: neurobasal medium (Life Technologies) supplemented with 6 mM Glutamax
304 (Life Technologies) and 1× B27 supplement (Life Technologies). Dissociated cells were seeded into
305 eight-well glass chamber slide (Matsunami Glass Ind., Osaka, Japan) coated with cell matrix type
306 IC (Nitta Gelatin Inc., Osaka, Japan). The cells propagated at 37°C and were used after 6−7 days of
307 culture. All animal experiments were approved by the President of Hokkaido University after
308 review by the Animal Care and Use Committee of Hokkaido University.
309
310 **Viruses**
311 The TBEV Oshima 5-10 strain was isolated from a dog in Hokuto City (Japan) in 1995
312 (AB062063.2) (Takashima *et al.*, 1997). The Sofjin-HO strain of TBEV was isolated from the brain
313 of a human patient in Khabarovsk (Russia) in 1937 (AB062064.1) (Zilber & Soloviev, 1946). The
314 Guriev strain of OHFV was isolated from human blood (AB507800). The recombinant viruses of
315 these strains were recovered from infectious cDNA clones as previously described (Hayasaka, 2004)
316 (Takano *et al.*, 2011) (Yoshii *et al.*, 2011). The WNV 6-LP strain was isolated from a New York City
317 isolate, NY99-6922 (AB185914.2). The WNV-6LP was propagated in a suckling mouse, and
318 passaged three times in BHK-21 cells and once in C6/36 cells. The JEV Sw/Mie40/2004 was
319 isolated from a pig (AB241118.1). The JEV Sw/Mie40/2004 was propagated in BHK-21 cells. The
320 Hochosterwitz strain of TBEV (unknown passage history) was isolated from an *Ixodes* tick in
321 Carinthia (Austria) in 1971 (KUNZ, 1981). The LGTV TP21 strain (unknown passage history) was

isolated from an *Ixodes* tick (AF253419.1). Working stocks of the all viruses were propagated once in BHK-21 cells, and stored at −80 °C. All viral infections were conducted in the BioSafety Level 3 conditions, in a dedicated laboratory located in the Graduate School of Veterinary Medicine of Hokkaido University.

Antibodies.

The following primary antibodies were used to perform IFA. Polyclonal mouse anti-LGTV (cross-reactive among the tick-borne flaviviruses), anti-WNV, and anti-JEV, antibodies were prepared from ascites of mice repeatedly immunized with LGTV TP21, WNV 6-LP, and JEV Ja-Gar01, respectively. These antibodies react with both structural and non-structural viral proteins, respectively (data not shown). Rabbit polyclonal antibodies, prepared by immunization with recombinant E and NS3 proteins derived from *Escherichia coli* as described previously (Yoshii *et al.*, 2004), were used to detect the TBEV E and NS3 proteins. The J2 mouse monoclonal antibody was used to detect the dsRNA, product of viral genome replication (English and Scientific Consulting, Szirak, Hungary). Chicken anti-MAP2, rabbit anti-GFAP, anti-β3 tubulin, and anti-synaptophysin polyclonal antibodies were the products of Abcam plc. (Cambridge, UK). Rabbit anti-calreticulin polyclonal antibodies were products of Affinity BioReagents, inc. (Golden, Colorado). The secondary antibodies, anti-mouse IgG, anti-rabbit IgG, and anti-chicken IgG conjugated with AlexaFluor488 or AlexaFluor555, were purchased from Life Technologies.

Construction of VLPs of TBEV

The plasmids Oshima REP (Hayasaka *et al.*, 2004) and pTBECME (Yoshii *et al.*, 2005) were used to construct VLPs of TBEV. The TBEV replicon was transcribed from the Oshima REP plasmid using a mMESSAGE mMACHINE SP6 kit (Life Technologies), and transfected into Human embryonic kidney 293T cells with the aid of a Trans IT mRNA transfection kit (Mirus Biology, Co.,

Madison, WI). After 5-6 h of culture, the cells were transfected with the pTBECME plasmid, which expresses the structural proteins of TBEV, with the aid of a TransIT-LT1 reagent (Mirus). The supernatant was harvested 48 h post-transfection and cleared by centrifugation at 17,000 g for 5 min. VLPs in the supernatant were precipitated by 10% (w/v) PEG 8000 and 1.9% (w/v) NaCl followed by incubation for 2 h at 4°C, and centrifugation at 16,000 g for 30 min. Pellets were resuspended in neurobasal medium and stored at −80°C.

Infection of primary neuronal cultures

Primary neuronal cultures were infected at an MOI of 0.1. After viral adsorption for 1 h, half of the culture medium was replaced. Medium was harvested at 12 h, 24 h, 48 h, 72 h post-infection (h.p.i.), and stored at −80°C. Cells were fixed and stained with toluidine blue, either subjected to IFA or viewed using TEM. Unless otherwise stated, TBEV Oshima 5-10 strain was used for TBEV infection.

Viral titration

Monolayers of BHK-21 cells, prepared in multi-well plates, were incubated with serial dilutions of viruses for 1 h, and next overlaid with minimum essential medium containing 2% (v/v) FBS and 1.5% (w/v) carboxymethyl cellulose. After 3−5 days of incubation, cells were fixed and stained with a solution of 0.25% (w/v) crystal violet in 10% (v/v) buffered formalin. Plaques were counted and viral titers expressed as plaque-forming unit (PFU)/ml.

Toluidine blue staining

After 48 h.p.i. of growth, infected primary neuronal cultures were fixed in 4% paraformaldehyde (w/v) for 20 min at 37°C, and next washed with 0.1 M glycine in PBS. Staining with toluidine blue followed, and images were viewed by using BZ-9000 fluorescence microscope (Keyence, Osaka,

372 Japan).

373

374 **IFA**

375 At 12−72 h.p.i., infected primary neuronal cultures were fixed in 4% (w/v) paraformaldehyde for 20
376 min at 37°C, and next washed with 0.1 M glycine in PBS. Fixed cells were permeabilized by
377 incubation in 0.1% (v/v) Triton X-100 for 5 min at room temperature, and next blocked with 2%
378 (w/v) bovine serum albumin. The cells were incubated at room temperature for 1 h with primary
379 antibodies. After extensive washing, cells were incubated with secondary antibodies bearing
380 fluorescent tags. The cells were enclosed with a solution of the Slowfade Gold antifade reagent with
381 DAPI (Life Technologies), and observed via BZ-9000 (Keyence) or LSM 700 confocal laser
382 scanning microscopy (Carl Zeiss Microscopy Co., Ltd., Jena, Germany). Images were processed
383 using the BZ-2 Analyser (Keyence) or ZEN 2009 (Carl Zeiss Microscopy) software.

384

385 **Cytoskeletal perturbation**

386 After viral adsorption for 1 h, half of the culture medium was exchanged, and nocodazole (final
387 concentration 5 μM) was added to the medium. The cells were fixed 48 h later, and effect of
388 cytoskeletal perturbation assessed using IFA.

389

390 **TEM**

391 Infected and mock-infected primary neuronal cultures growing in eight-chambered slides were
392 directly pre-fixed overnight with a solution of 2.5% (w/v) glutaraldehyde and 2% (w/v)
393 paraformaldehyde in 0.1 M phosphate buffer, at 4°C. After washing with 0.1 M phosphate buffer,
394 cells were post-fixed in 1% (w/v) osmium tetroxide and dehydrated in a graded series of alcohol.
395 Cells were next embedded in a Quetol 812, DDSA, and MNA mixture (Nisshin EM, Tokyo, Japan).
396 Ultrathin sections were stained with uranyl acetate and lead citrate and visualized via JEM-1400plus

(JEOL Ltd., Tokyo, Japan).

Acknowledgments

This work was supported by Grants-in-Aid for Scientific Research (24780293, 22780268 and 21405035) and the global COE program from the Ministry of Education, Culture, Sports, Sciences and Technology of Japan, and Health Sciences Grants for Research on Emerging and Re-emerging Infectious Disease from Ministry of Health, Labour and Welfare of Japan.

References

Anastasiadou, A., Kakoulidis, I., Butel, D., Kehagia, E. & Papa, A. (2013). Follow-up study of Greek patients with West Nile virus neuroinvasive disease. *Int J Infect Dis* **17**, E494-E497.

Bagni, C. & Greenough, W. T. (2005). From mRNP trafficking to spine dysmorphogenesis: the roots of fragile X syndrome. *Nature reviews Neuroscience* **6**, 376-387.

Balogh, Z., Ferenczi, E., Szeles, K., Stefanoff, P., Gut, W., Szomor, K. N., Takacs, M. & Berencsi, G. (2010). Tick-borne encephalitis outbreak in Hungary due to consumption of raw goat milk. *Journal of Virological Methods* **163**, 481-485.

Banker, G. A. & Cowan, W. M. (1977). Rat hippocampal neurons in dispersed cell culture. *Brain research* **126**, 397-342.

Baumann, N. & Pham-Dinh, D. (2001). Biology of oligodendrocyte and myelin in the mammalian central nervous system. *Physiological reviews* **81**, 871-927.

Biederer, T. & Scheiffele, P. (2007). Mixed-culture assays for analyzing neuronal synapse formation. *Nature protocols* **2**, 670-676.

Billoir, F., de Chesse, R., Tolou, H., de Micco, P., Gould, E. A. & de Lamballerie, X. (2000). Phylogeny of the genus flavivirus using complete coding sequences of arthropod-borne viruses and viruses with no known vector. *The Journal of general virology* **81 Pt 9**, 2339.

Bramham, C. R. & Wells, D. G. (2007). Dendritic mRNA: transport, translation and function. *Nature reviews Neuroscience* **8**, 776-789.

Calon, F., Lim, G. P., Yang, F. S., Morihara, T., Teter, B., Ubeda, O., Rostaing, P., Triller, A., Salem, N., Ashe, K. H., Frautschy, S. A. & Cole, G. M. (2004). Docosahexaenoic acid protects from dendritic pathology in an Alzheimer's disease mouse model. *Neuron* **43**, 633-645.

Chambers, T. J., Hahn, C. S., Galler, R. & Rice, C. M. (1990). Flavivirus genome organization, expression, and replication. *Annual review of microbiology* **44**, 649-688.

Chen, C. J., Ou, Y. C., Chang, C. Y., Pan, H. C., Lin, S. Y., Liao, S. L., Raung, S. L., Chen, S. Y. & Chang, C. J. (2011). Src signaling involvement in Japanese encephalitis virus-induced cytokine production in microglia. *Neurochemistry international* **58**, 924-933.

Chen, C. J., Ou, Y. C., Lin, S. Y., Raung, S. L., Liao, S. L., Lai, C. Y., Chen, S. Y. & Chen, J. H. (2010). Glial activation involvement in neuronal death by Japanese encephalitis virus infection. *Journal of General Virology* **91**, 1028-1037.

Cho, H., Proll, S. C., Szretter, K. J., Katze, M. G., Gale, M., Jr. & Diamond, M. S. (2013). Differential innate immune response programs in neuronal subtypes determine susceptibility to infection in the brain by positive-stranded RNA viruses. *Nature medicine* **19**, 458-464.

Chung, W. M., Buseman, C. M., Joyner, S. N., Hughes, S. M., Fomby, T. B., Luby, J. P. & Haley, R. W. (2013). The

2012 West Nile encephalitis epidemic in Dallas, Texas. *JAMA : the journal of the American Medical Association* **310**, 297-307.

Comery, T. A., Harris, J. B., Willems, P. J., Oostra, B. A., Irwin, S. A., Weiler, I. J. & Greenough, W. T. (1997). Abnormal dendritic spines in fragile X knockout mice: Maturation and pruning deficits. *Proceedings of the National Academy of Sciences of the United States of America* **94**, 5401-5404.

Consortium, T. D.-B. F. X. (1994). Fmr1 knockout mice: a model to study fragile X mental retardation. The Dutch-Belgian Fragile X Consortium. *Cell* **78**, 23-33.

Cook, S., Moureau, G., Kitchen, A., Gould, E. A., de Lamballerie, X., Holmes, E. C. & Harbachl, R. E. (2012). Molecular evolution of the insect-specific flaviviruses. *Journal of General Virology* **93**, 223-234.

Crabtree, M. B., Sang, R. C., Stollar, V., Dunster, L. M. & Miller, B. R. (2003). Genetic and phenotypic characterization of the newly described insect flavivirus, Kamiti River virus. *Archives of virology* **148**, 1095-1118.

Czupryna, P., Moniuszko, A., Pancewicz, S. A., Grygorczuk, S., Kondrusik, M. & Zajkowska, J. (2011). Tick-borne encephalitis in Poland in years 1993-2008-epidemiology and clinical presentation. A retrospective study of 687 patients. *Eur J Neurol* **18**, 673-679.

Danis, K., Papa, A., Theocharopoulos, G., Dougas, G., Athanasiou, M., Detsis, M., Baka, A., Lytras, T., Mellou, K., Bonovas, S. & Panagiotopoulos, T. (2011). Outbreak of West Nile virus infection in Greece, 2010. *Emerging infectious diseases* **17**, 1868-1872.

Desai, A., Shankar, S. K., Ravi, V., Chandramuki, A. & Gouriedevi, M. (1995). JAPANESE ENCEPHALITIS-VIRUS ANTIGEN IN THE HUMAN BRAIN AND ITS TOPOGRAPHIC DISTRIBUTION. *Acta neuropathologica* **89**, 368-373.

Diniz, J. A. P., Da Rosa, A., Guzman, H., Xu, F. L., Xiao, S. Y., Popov, V. L., Vasconcelos, P. F. C. & Tesh, R. B. (2006). West Nile virus infection of primary mouse neuronal and neuroglial cells: The role of astrocytes in chronic infection. *Am J Trop Med Hyg* **75**, 691-696.

Gehrke, R., Ecker, M., Aberle, S. W., Allison, S. L., Heinz, F. X. & Mandl, C. W. (2003). Incorporation of tick-borne encephalitis virus replicons into virus-like particles by a packaging cell line. *Journal of virology* **77**, 8924-8933.

Gelpi, E., Preusser, M., Garzuly, F., Holzmann, H., Heinz, F. X. & Budka, H. (2005). Visualization of central European tick-borne encephalitis infection in fatal human cases. *Journal of neuropathology and experimental neurology* **64**, 506-512.

German, A. C., Myint, K. S. A., Mai, N. T. H., Pomeroy, I., Phu, N. H., Tzartos, J., Winter, P., Collett, J., Farrar, J., Barrett, A., Kipar, A., Esiri, M. M. & Solomon, T. (2006). A preliminary neuropathological study of Japanese encephalitis in humans and a mouse model. *Transactions of the Royal Society of Tropical Medicine and Hygiene* **100**, 1135-1145.

Gould, E. A. & Solomon, T. (2008). Pathogenic flaviviruses. *Lancet* **371**, 500-509.

Hayasaka, D. (2004). Amino acid changes responsible for attenuation of virus neurovirulence in an infectious cDNA clone of the Oshima strain of Tick-borne encephalitis virus. *Journal of General Virology* **85**, 1007-1018.

Hayasaka, D., Nagata, N., Fujii, Y., Hasegawa, H., Sata, T., Suzuki, R., Gould, E. A., Takashima, I. & Koike, S. (2009). Mortality following peripheral infection with Tick-borne encephalitis virus results from a combination

of central nervous system pathology, systemic inflammatory and stress responses. *Virology* **390**, 139-150.

Hayasaka, D., Yoshii, K., Ueki, T., Iwasaki, T. & Takashima, I. (2004). Sub-genomic replicons of Tick-borne encephalitis virus. *Archives of virology* **149**, 1245-1256.

Hussmann, K. L., Samuel, M. A., Kim, K. S., Diamond, M. S. & Fredericksen, B. L. (2013). Differential replication of pathogenic and nonpathogenic strains of West Nile virus within astrocytes. *Journal of virology* **87**, 2814-2822.

Ishihara, N., Nomura, M., Jofuku, A., Kato, H., Suzuki, S. O., Masuda, K., Otera, H., Nakanishi, Y., Nonaka, I., Goto, Y. I., Taguchi, N., Morinaga, H., Maeda, M., Takayanagi, R., Yokota, S. & Mihara, K. (2009). Mitochondrial fission factor Drp1 is essential for embryonic development and synapse formation in mice. *Nature Cell Biology* **11**, 958-U114.

Kaiser, R. (1999). The clinical and epidemiological profile of tick-borne encephalitis in southern Germany 1994-98 - A prospective study of 656 patients. *Brain* **122**, 2067-2078.

Kanai, Y., Dohmae, N. & Hirokawa, N. (2004). Kinesin transports RNA: isolation and characterization of an RNA-transporting granule. *Neuron* **43**, 513-525.

Khromykh, A. A., Varnavski, A. N. & Westaway, E. G. (1998). Encapsidation of the flavivirus kunjin replicon RNA by using a complementation system providing Kunjin virus structural proteins in trans. *Journal of virology* **72**, 5967-5977.

Kiebler, M. A. & DesGroseillers, L. (2000). Molecular insights into mRNA transport and local translation in the mammalian nervous system. *Neuron* **25**, 19-28.

Kimura, T., Sasaki, M., Okumura, M., Kim, E. & Sawa, H. (2010). Flavivirus Encephalitis: Pathological Aspects of Mouse and Other Animal Models. *Veterinary pathology* **47**, 806-818.

Kohrmann, M., Luo, M., Kaether, C., DesGroseillers, L., Dotti, C. G. & Kiebler, M. A. (1999). Microtubule-dependent recruitment of Staufen-Green fluorescent protein into large RNA-containing granules and subsequent dendritic transport in living hippocampal neurons. *Molecular biology of the cell* **10**, 2945-2953.

Kuno, G., Chang, G. J., Tsuchiya, K. R., Karabatsos, N. & Cropp, C. B. (1998). Phylogeny of the genus Flavivirus. *Journal of virology* **72**, 73-83.

KUNZ, F. X. H. C. (1981). Homogeneity of the Structural Glycoprotein from European Isolates of Tick-borne Encephalitis Virus: Comparison with Other Flaviviruses. *J gen Virol*.

Lewis, P. & Lentz, T. L. (1998). Rabies virus entry into cultured rat hippocampal neurons. *Journal of neurocytology* **27**, 559-573.

Li, X. Q., Sarmento, L. & Fu, Z. F. (2005). Degeneration of neuronal processes after infection with pathogenic, but not attenuated, rabies viruses. *Journal of virology* **79**, 10063-10068.

Lindenbach, B. D. T. H. R., C.M. (2007). Flaviviridae: The viruses and their replication, in Fields Virology, 5th edn. *Fields Virology 5th edn*, 1101-1152.

Lindquist, L. & Vapalahti, O. (2008). Tick-borne encephalitis. *Lancet* **371**, 1861-1871.

Mackenzie, J. (2005). Wrapping things up about virus RNA replication. *Traffic* **6**, 967-977.

Mackenzie, J. S., Gubler, D. J. & Petersen, L. R. (2004). Emerging flaviviruses: the spread and resurgence of Japanese encephalitis, West Nile and dengue viruses. *Nature medicine* **10**, S98-109.

Mackenzie, J. S. & Williams, D. T. (2009). The Zoonotic Flaviviruses of Southern, South-Eastern and Eastern Asia, and Australasia: The Potential for Emergent Viruses. *Zoonoses and Public Health* **56**, 338-356.

Maezawa, I. & Jin, L. W. (2010). Rett Syndrome Microglia Damage Dendrites and Synapses by the Elevated Release of Glutamate. *Journal of Neuroscience* **30**, 5346-5356.

Martone, M. E., Zhang, Y., Simpliciano, V. M., Carragher, B. O. & Ellisman, M. H. (1993). Three-dimensional visualization of the smooth endoplasmic reticulum in Purkinje cell dendrites. *The Journal of neuroscience : the official journal of the Society for Neuroscience* **13**, 4636-4646.

Matsuda, K., Shibata, T., Sakoda, Y., Kida, H., Kimura, T., Ochiai, K. & Umemura, T. (2005). In vitro demonstration of neural transmission of avian influenza A virus. *The Journal of general virology* **86**, 1131-1139.

McCarthy, J. B. & Milner, T. A. (2003). Dendritic ribosomes suggest local protein synthesis during estrous synaptogenesis. *Neuroreport* **14**, 1357-1360.

McMichael, A. J., Woodruff, R. E. & Hales, S. (2006). Climate change and human health: present and future risks. *Lancet* **367**, 859-869.

Mickiene, A., Laiskonis, A., Gunther, G., Vene, S., Lundkvist, A. & Lindquist, L. (2002). Tickborne encephalitis in an area of high endemicity in lithuania: Disease severity and long-term prognosis. *Clin Infect Dis* **35**, 650-658.

Molenkamp, R., Kooi, E. A., Lucassen, M. A., Greve, S., Thijssen, J. C. P., Spaan, W. J. M. & Bredenbeek, P. J. (2003). Yellow fever virus replicons as an expression system for hepatitis C virus structural proteins. *Journal of virology* **77**, 1644-1648.

Morse, S. S. (1995). Factors in the emergence of infectious diseases. *Emerging infectious diseases* **1**, 7-15.

Muramatsu, T., Ohmae, A. & Anzai, K. (1998). BC1 RNA protein particles in mouse brain contain two Y-, H-element-binding proteins, translin and a 37 kDa protein. *Biochemical and biophysical research communications* **247**, 7-11.

Okabe, S. (2013). Fluorescence imaging of synapse formation and remodeling. *Journal of electron microscopy* **62**, 51-62.

Omalu, B. I., Shakir, A. A., Wang, G. J., Lipkin, W. I. & Wiley, C. A. (2003). Fatal fulminant pan-meningo-polioencephalitis due to West Nile virus. *Brain Pathology* **13**, 465-472.

Ooi, M. H., Lewthwaite, P., Lai, B. F., Mohan, A., Clear, D., Lim, L., Krishnan, S., Preston, T., Chieng, C. H., Tio, P. H., Wong, S. C., Cardosa, J. & Solomon, T. (2008). The epidemiology, clinical features, and long-term prognosis of Japanese encephalitis in Central Sarawak, Malaysia, 1997-2005. *Clin Infect Dis* **47**, 458-468.

Ori-McKenney, K. M., Jan, L. Y. & Jan, Y. N. (2012). Golgi outposts shape dendrite morphology by functioning as sites of acentrosomal microtubule nucleation in neurons. *Neuron* **76**, 921-930.

Perkins, D., Pereira, E. F., Gober, M., Yarowsky, P. J. & Aurelian, L. (2002). The herpes simplex virus type 2 R1 protein kinase (ICP10 PK) blocks apoptosis in hippocampal neurons, involving activation of the MEK/MAPK survival pathway. *Journal of virology* **76**, 1435-1449.

Pierce, J. P., Mayer, T. & McCarthy, J. B. (2001). Evidence for a satellite secretory pathway in neuronal dendritic spines. *Current Biology* **11**, 351-355.

Ramirez, O. A. & Couve, A. (2011). The endoplasmic reticulum and protein trafficking in dendrites and axons. *Trends in cell biology* **21**, 219-227.

Reynard, O., Mokhonov, V., Mokhonova, E., Leung, J., Page, A., Mateo, M., Pyankova, O., Georges-Courbot, M. C., Raoul, H., Khromykh, A. A. & Volchkov, V. E. (2011). Kunjin virus replicon-based vaccines expressing Ebola virus glycoprotein GP protect the guinea pig against lethal Ebola virus infection. *The Journal of infectious diseases* **204 Suppl 3**, S1060-1065.

Roche, J. P., Packard, M. C., Moeckel-Cole, S. & Budnik, V. (2002). Regulation of synaptic plasticity and synaptic vesicle dynamics by the PDZ protein scribble. *Journal of Neuroscience* **22**, 6471-6479.

Ruzek, D., Vancova, M., Tesarova, M., Ahantarig, A., Kopecky, J. & Grubhoffer, L. (2009). Morphological changes in human neural cells following tick-borne encephalitis virus infection. *The Journal of general virology* **90**, 1649-1658.

Schmaljohn, A. L. & McClain, D. (1996). Alphaviruses (Togaviridae) and Flaviviruses (Flaviviridae). In *Medical Microbiology*, 4th edn. Edited by S. Baron. Galveston (TX).

Sejvar, J. J., Haddad, M. B., Tierney, B. C., Campbell, G. L., Marfin, A. A., Van Gerpen, J. A., Fleischauer, A., Leis, A. A., Stokic, D. S. & Petersen, L. R. (2003). Neurologic manifestations and outcome of West Nile virus infection. *JAMA-J Am Med Assoc* **290**, 511-515.

Sinnamon, J. R. & Czaplinski, K. (2011). mRNA trafficking and local translation: the Yin and Yang of regulating mRNA localization in neurons. *Acta Biochimica Et Biophysica Sinica* **43**, 663-670.

Solomon, T., Kneen, R., Dung, N. M., Khanh, V. G., Thuy, T. T. N., Ha, D. Q., Day, N. P. J., Nisalak, A., Vaughn, D. W. & White, N. J. (1998). Poliomyelitis-like illness due to Japanese encephalitis virus. *Lancet* **351**, 1094-1097.

Steward, O. & Schuman, E. M. (2003). Compartmentalized synthesis and degradation of proteins in neurons. *Neuron* **40**, 347-359.

Takano, A., Yoshii, K., Omori-Urabe, Y., Yokozawa, K., Kariwa, H. & Takashima, I. (2011). Construction of a replicon and an infectious cDNA clone of the Sofjin strain of the Far-Eastern subtype of tick-borne encephalitis virus. *Archives of virology* **156**, 1931-1941.

Takashima, I., Morita, K., Chiba, M., Hayasaka, D., Takezawa, T. S. C., Kariwa, A. I. H., Yoshimatsu, K., Arikawa, J. & Hashimoto, N. (1997). A case of tick-borne encephalitis in Japan and isolation of the the virus. *Journal of clinical microbiology*.

Uchil, P. D. & Satchidanandam, V. (2003). Architecture of the flaviviral replication complex. Protease, nuclease, and detergents reveal encasement within double-layered membrane compartments. *The Journal of biological chemistry* **278**, 24388-24398.

Viesselmann, C., Ballweg, J., Lumbard, D. & Dent, E. W. (2011). Nucleofection and primary culture of embryonic mouse hippocampal and cortical neurons. *Journal of visualized experiments : JoVE*.

Vong, S., Khieu, V., Glass, O., Ly, S., Duong, V., Huy, R., Ngan, C., Wichmann, O., Letson, G. W., Margolis, H. S. & Buchy, P. (2010). Dengue incidence in urban and rural Cambodia: results from population-based active fever surveillance, 2006-2008. *PLoS neglected tropical diseases* **4**, e903.

Wang, X. L., Su, B., Lee, H. G., Li, X. Y., Perry, G., Smith, M. A. & Zhu, X. W. (2009). Impaired Balance of Mitochondrial Fission and Fusion in Alzheimer's Disease. *Journal of Neuroscience* **29**, 9090-9103.

Welsch, S., Miller, S., Romero-Brey, I., Merz, A., Bleck, C. K. E., Walther, P., Fuller, S. D., Antony, C., Krijnse-Locker, J. & Bartenschlager, R. (2009). Composition and Three-Dimensional Architecture of the

Dengue Virus Replication and Assembly Sites. *Cell host & microbe* **5**, 365-375.

Wigerius, M., Melik, W., Elvang, A. & Johansson, M. (2010). Rac1 and Scribble are targets for the arrest of neurite outgrowth by TBE virus NS5. *Molecular and Cellular Neuroscience* **44**, 260-271.

Xiao, S. Y., Guzman, H., Zhang, H., da Rosa, A. & Tesh, R. B. (2001). West Nile Virus infection in the golden hamster (Mesocricetus auratus): A model for West Nile encephalitis. *Emerging infectious diseases* **7**, 714-721.

Yoshii, K., Goto, A., Kawakami, K., Kariwa, H. & Takashima, I. (2008). Construction and application of chimeric virus-like particles of tick-borne encephalitis virus and mosquito-borne Japanese encephalitis virus. *The Journal of general virology* **89**, 200-211.

Yoshii, K., Hayasaka, D., Goto, A., Kawakami, K., Kariwa, H. & Takashima, I. (2005). Packaging the replicon RNA of the Far-Eastern subtype of tick-borne encephalitis virus into single-round infectious particles: development of a heterologous gene delivery system. *Vaccine* **23**, 3946-3956.

Yoshii, K., Igarashi, M., Ito, K., Kariwa, H., Holbrook, M. R. & Takashima, I. (2011). Construction of an infectious cDNA clone for Omsk hemorrhagic fever virus, and characterization of mutations in NS2A and NS5. *Virus research* **155**, 61-68.

Yoshii, K., Konno, A., Goto, A., Nio, J., Obara, M., Ueki, T., Hayasaka, D., Mizutani, T., Kariwa, H. & Takashima, I. (2004). Single point mutation in tick-borne encephalitis virus prM protein induces a reduction of virus particle secretion. *The Journal of general virology* **85**, 3049-3058.

Zilber, L. & Soloviev, V. (1946). Far Eastern tick-borne springsummer (spring) encephalitis. *Am Rev Sov Med*.

Figure legends

Fig. 1. Virus production in primary neuronal cell cultures

(a) TBEV growth kinetics in primary cell cultures. Hippocamal (closed circles), cerebral cortex (crosses), and cerebellal (open triangles) cells were infected with TBEV at an MOI of 0.1 and, at the indicated time points, the media were harvested and virus titers determined by plaque forming assay. Error bars: standard deviations.

(b) Virus production levels in primary cultures of cells from various brain regions. Cells from the hippocampus (Hip), cerebral cortex (Cor), and cerebellum (Cer) were infected with TBEV, WNV, or JEV at an MOI of 0.1. Virus titers in supernatants at 48 h.p.i. were measured.

(c) Infected neurons were stained with toluidine blue. Cultured cerebral cortex cells were infected with TBEV or WNV at an MOI of 0.1. Infected cells and mock-infected cells were fixed at 48 h.p.i. and stained with toluidine blue. Scale bars: 50 μm.

Fig. 2. Distribution of viral antigens and MAP2 in primary neuronal cultures

(a) Viral antigen distribution at 48 h.p.i.. Cultured cerebral cortex cells were infected with TBEV (i−v), WNV (vi−x), or JEV (xi−xv), at an MOI of 0.1. The infected cells were fixed at 48 h.p.i., and stained with antibodies against MAP2 (green), antisera against each virus (red), and DAPI (blue). Panels (iv, v, ix, x, ixv, and xv) show magnifications of dendrites from the indicated regions of the merged images. Scale bars: 50 μm.

(b) Viral protein accumulations in TBEV-infected dendrites. Infected cells were fixed at 48 h.p.i. and stained with antibodies against MAP2 (green) and an antiserum against a tick-borne flaviviruses (red). The images were collected with a confocal laser scanning microscopy. Panels (termed Region1: ii−iv, and Region2: v−vii) show magnifications of dendrites in the indicated region of panel (i).

Accumulations of viral antigens in dendrites are indicated by white arrows.

Fig. 3. Time-course changes in viral antigen distribution

(a) IFA images showing the changes over time in viral antigen distributions in primary neuronal cultures. Cultured cerebral cortex cells were infected with TBEV (i−iv), WNV (v−viii), or JEV (ix−xii) at an MOI of 0.1. The infected cells were fixed at the indicated time points (12, 24, 48, and 72 h.p.i.), and stained with antisera against each virus (red). Accumulations of viral antigens are indicated by white arrows. Scale bars: 50 μm.

(b) The extent of viral antigen accumulations in infected cells. Cultured cerebral cortex cells were infected with TBEV, WNV, or JEV at an MOI of 0.1., fixed the indicated timepoints (12, 24, 48, and 72 h.p.i.), and stained with antisera against each virus and DAPI. The numbers of infected cells and antigen accumulationsins in such cells were counted in four different microscopic fields. Error bars: standard deviation. **: $P<0.01$ by Tukey's test.

Fig. 4. Co-staining of TBEV-antigen and cellular organelles

Neuronal cells were mock-infected (a-d) or infected with TBEV (e-ab) at an MOI of 0.1, and fixed at 48 h.p.i.. The cells were stained with antibodies against organelle markers (green), an antiserum against tick-borne flaviviruses (red), and DAPI (blue). Antibodies against MAP2 (a and e−j), β3-tublin (b and k−p), carleticulin (c and q-v), and synaptophysin (d and w-ab) were used as organelle markers. The accumulations of viral antigens are magnified in panels (h−j, n−p, t-v, and z−ab). Accumulations of viral antigens are indicated by white arrows. Scale bars: 50 μm.

Fig. 5. Effect of microtubule perturbation on viral antigen distribution

Cells were mock-infected (a−c) or infected with TBEV (d−f) or WNV (g−i) at an MOI of 0.1, and treated with nocodazole. The infected cells were fixed at 48 h.p.i. and stained with antibodies against

MAP2 (green), antisera against each virus (red), and DAPI (blue). Scale bars: 50 μm.

Fig. 6. Viral constituents present in antigen accumulations in dendrites

(a) Cells were infected with TBEV at an MOI of 0.1, and fixed at 72 h.p.i.. The fixed cells were stained with antibodies against viral proteins (green), an antiserum against a tick-borne flaviviruses (red), and DAPI (blue). Two antibodies targeting E protein (i−iii) and NS3 (iv−vi) were used. Scale bars: 50 μm.

(b) Cells were infected with TBEV at an MOI of 0.1, and fixed at 48 h.p.i.. The fixed cells were stained with antibodies against the TBEV E protein (green), an antibody against dsRNA (red), and DAPI (blue). The accumulation of viral antigens is magnified in panels (ii-iv). The images were collected with a confocal laser scanning microscopy.

(c) Cells were infected with VLPs of TBEV and fixed at 48 h.p.i.. Neurons were stained with an antibody against MAP2 (green), an antiserum against a tick-borne flaviviruses (red), and DAPI (blue). Accumulations of viral antigens are magnified in panels (iv and v). Scale bars: 50 μm.

Accumulations of viral antigens are indicated by white arrows.

Fig. 7. Ultrastructural changes in primary neuronal cultures upon flaviviral infection

Primary neuronal cultures were examined by TEM; these included mock-infected cells (a−c, and f), cells infected with TBEV (d, e, and h−l), and cells infected with WNV (g). **(a−c)** Mock-infected neurons contained structurally intact organelles (Nu: Nucleus, Cyto: Cytosol, ER: endoplasmic reticulum, and Mit: Mitochondria). **(d)** TBEV infected neurons exhibited cytoplasmic condensation, and reactive lysosomes were also observed (Lys: Lysosome). **(e)** Virion-like structures coated with lipid bilayers were evident (white arrows). **(f)** Normal microtubule structure was observed in mock infected neurites. **(g)** WNV triggered degeneration of membrane structure (white arrowhead) and the appearance of granular aggregates in the neurites. **(h)** TBEV infection triggered swelling of and

development of elliptical membrane-encased structures in neurites. **(i)** A laminal membrane structure was observed adjacent to microtubules. **(j-l)** Representative images of the regions (surrounding those shown in h, and i). Virion-like structures coated with lipid bilayers were observed both inside and outside the observed structures (white arrows).

Fig. 8. Schematic diagram of LMS formation and the contribution thereof to neuro-pathogenicity

(a) Viral proteins are synthesized by free ribosomes in the dendrites. **(b)** Synthesized proteins form the LMS by modulating the structure of host-membranes. **(c)** The LMS becomes enlarged and compromises microtubule linearity, thus obstructing trafficking pathways.

The English in this document has been checked by at least two professional editors, both native speakers of English. For a certificate, please see:

http://www.textcheck.com/certificate/vOO0vI

Fig. 1

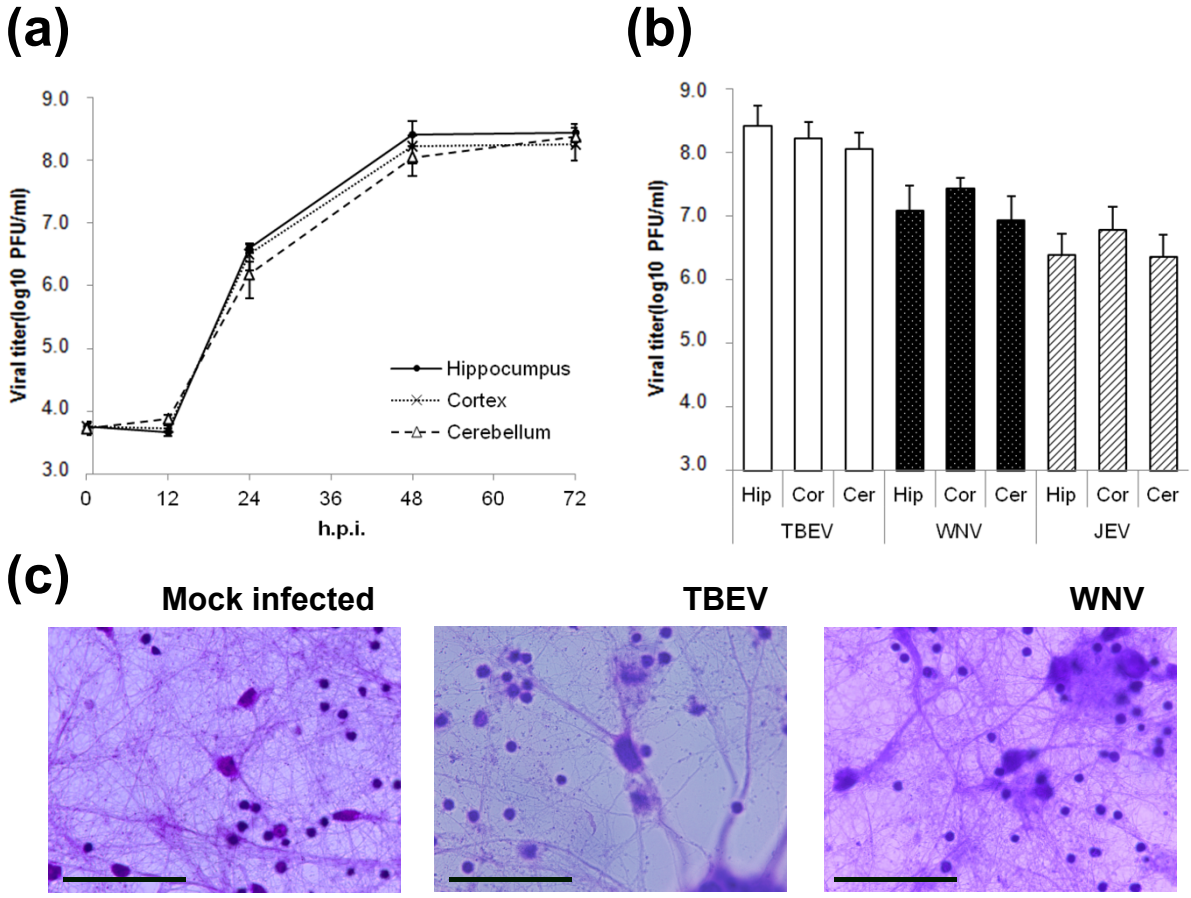
(a)
Viral titer(log10 PFU/ml)
9.0
8.0
7.0
6.0
5.0
4.0
3.0
0
12
24
36
48
60
72
h.p.i.
Hippocumpus
Cortex
Cerebellum
(b)
Viral titer(log10 PFU/ml)
9.0
8.0
7.0
6.0
5.0
4.0
3.0
Hip
Cor
Cer
Hip
Cor
Cer
Hip
Cor
Cer
TBEV
WNV
JEV
(c)
Mock infected
TBEV
WNV

Fig. 2

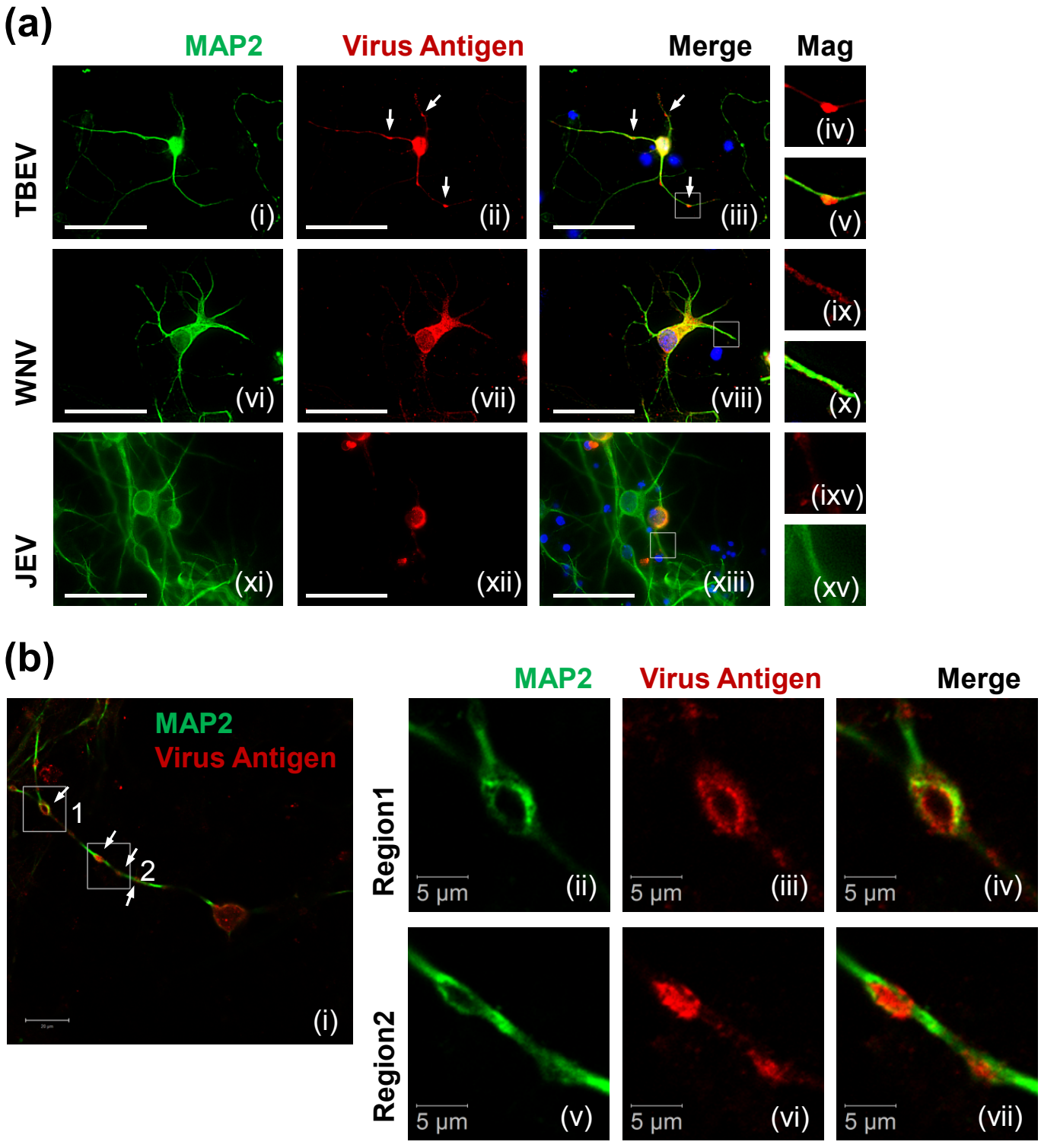
(a)
MAP2
Virus Antigen
Merge
Mag
TBEV
WNV
JEV
(i)
(ii)
(iii)
(iv)
(v)
(vi)
(vii)
(viii)
(ix)
(x)
(xi)
(xii)
(xiii)
(ixv)
(xv)
(b)
MAP2
Virus Antigen
1
2
(i)
Region1
Region2
MAP2
Virus Antigen
Merge
5 μm
(ii)
(iii)
(iv)
(v)
(vi)
(vii)

Fig. 3

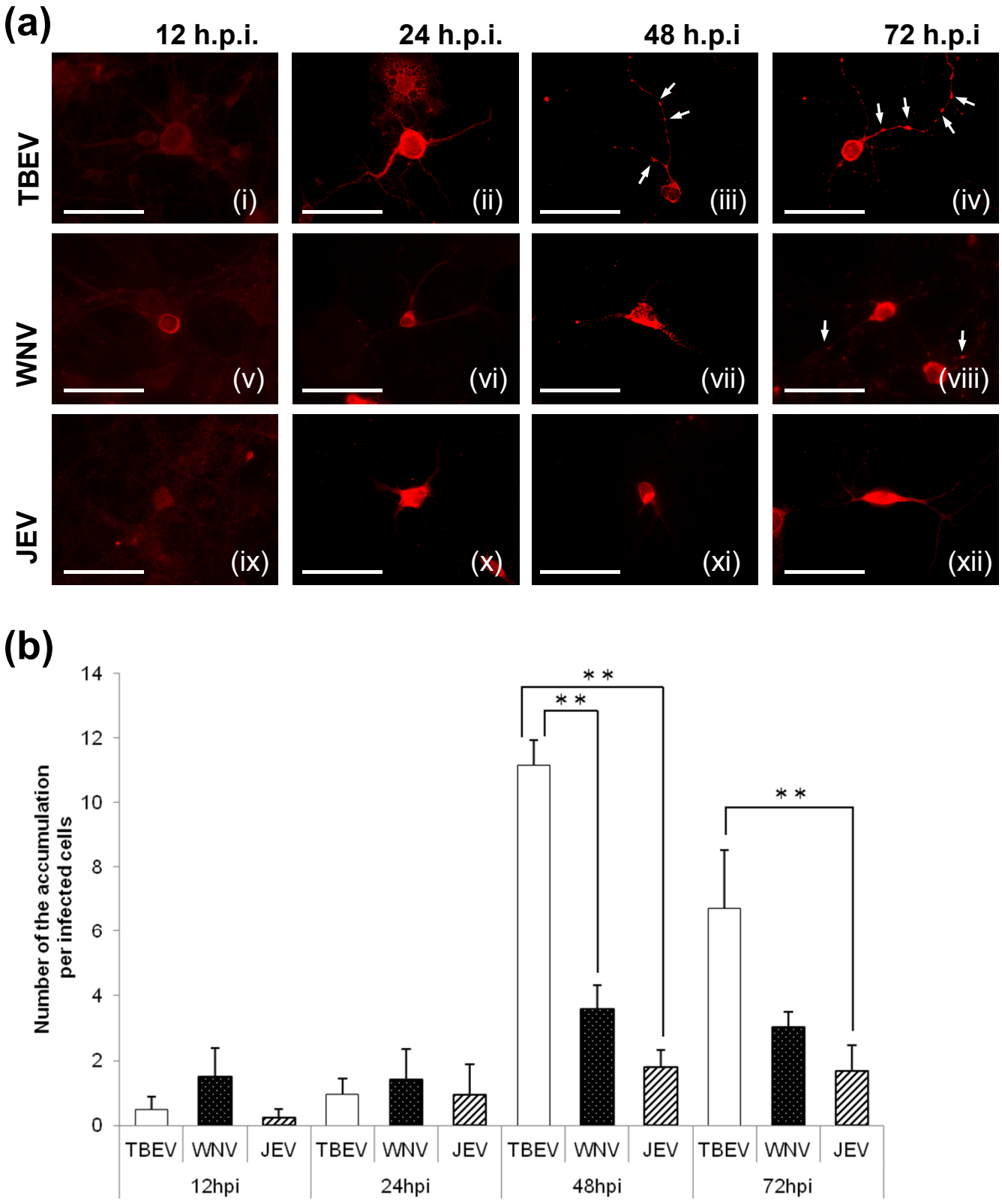
(a)
12 h.p.i.
24 h.p.i.
48 h.p.i
72 h.p.i
TBEV
WNV
JEV
(i)
(ii)
(iii)
(iv)
(v)
(vi)
(vii)
(viii)
(ix)
(x)
(xi)
(xii)
(b)
Number of the accumulation per infected cells
0
2
4
6
8
10
12
14
* *
* *
* *
TBEV
WNV
JEV
12hpi
24hpi
48hpi
72hpi

Fig. 4

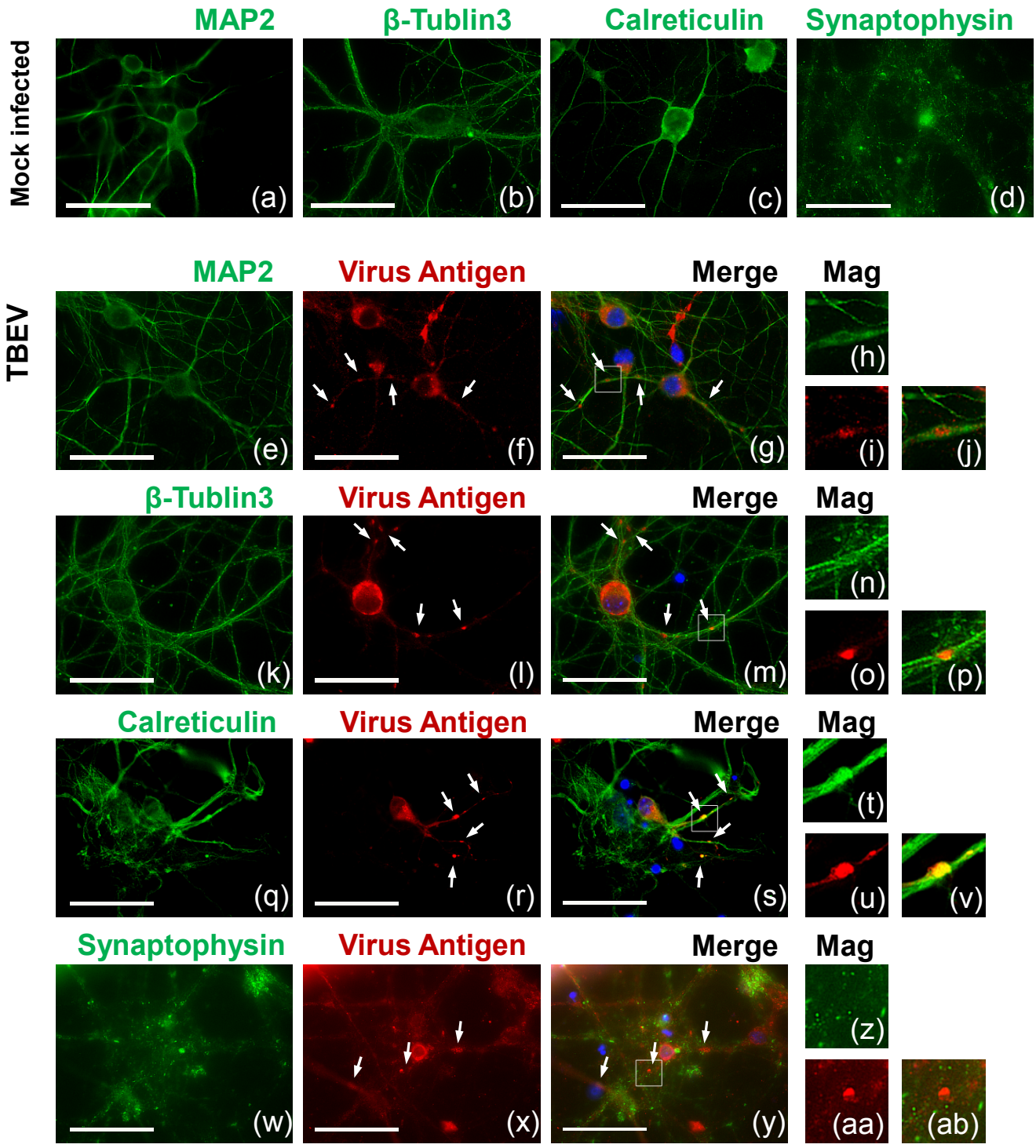
Mock infected
MAP2
β-Tublin3
Calreticulin
Synaptophysin
(a)
(b)
(c)
(d)
TBEV
MAP2
Virus Antigen
Merge
Mag
(e)
(f)
(g)
(h)
(i)
(j)
β-Tublin3
Virus Antigen
Merge
Mag
(k)
(l)
(m)
(n)
(o)
(p)
Calreticulin
Virus Antigen
Merge
Mag
(q)
(r)
(s)
(t)
(u)
(v)
Synaptophysin
Virus Antigen
Merge
Mag
(w)
(x)
(y)
(z)
(aa)
(ab)

Fig. 5

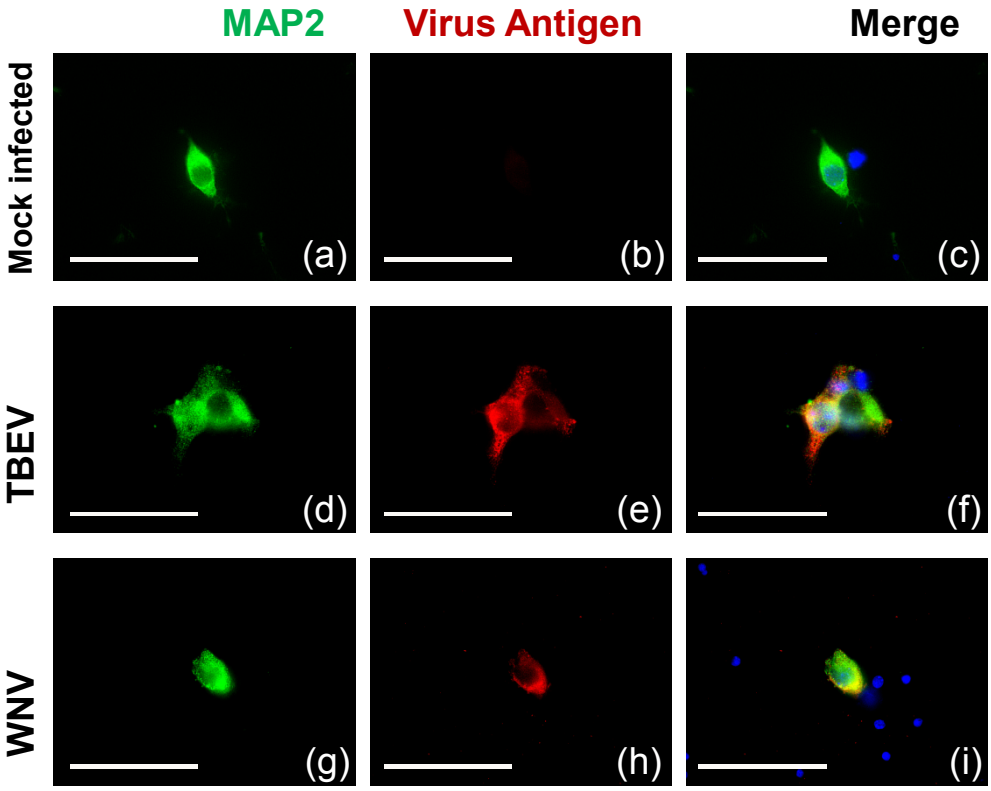

Fig. 6

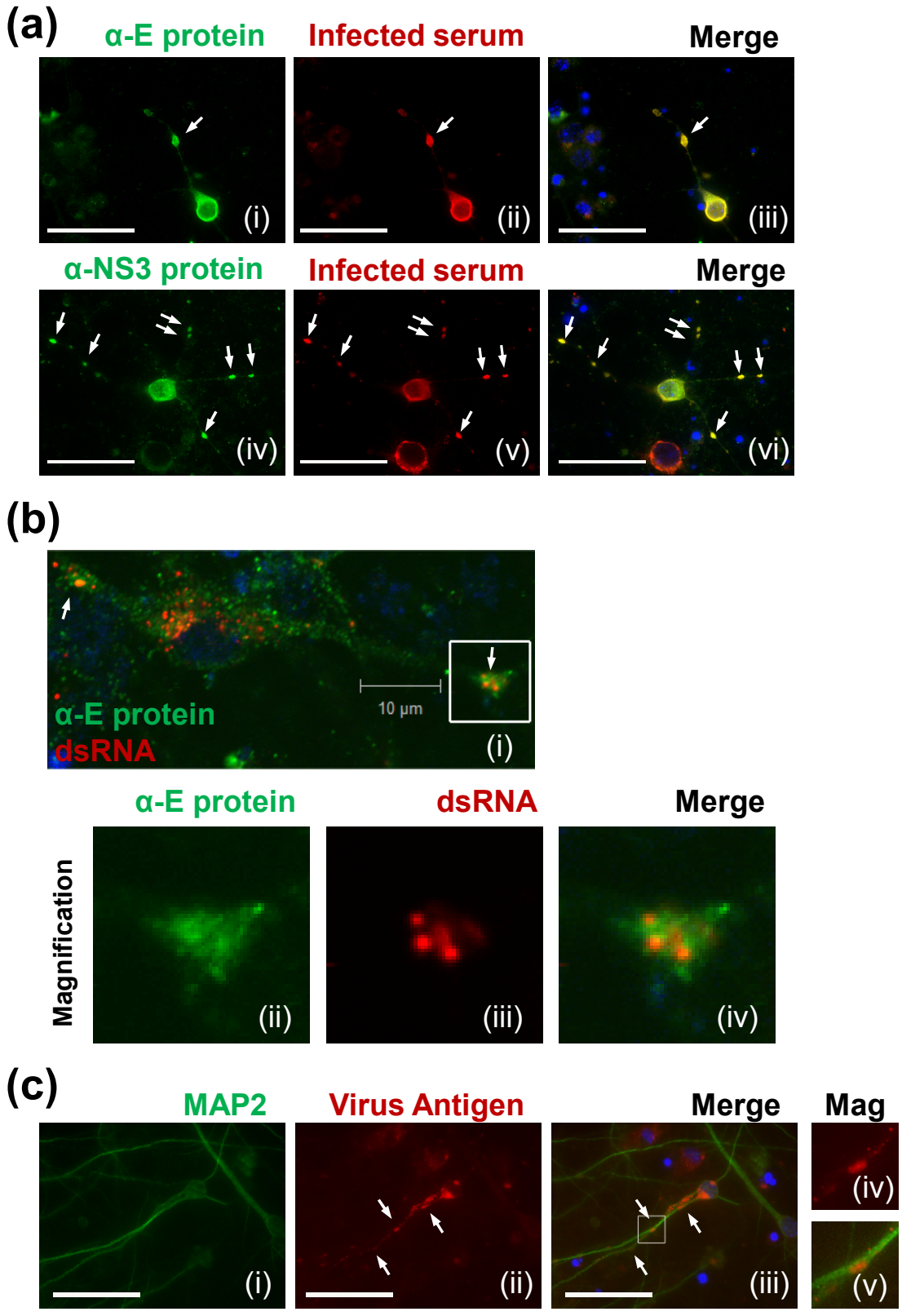
(a)
α-E protein
Infected serum
Merge
(i)
(ii)
(iii)
α-NS3 protein
Infected serum
Merge
(iv)
(v)
(vi)
(b)
α-E protein
dsRNA
10 μm
(i)
α-E protein
dsRNA
Merge
Magnification
(ii)
(iii)
(iv)
(c)
MAP2
Virus Antigen
Merge
Mag
(i)
(ii)
(iii)
(iv)
(v)

Fig. 7 (1/2)

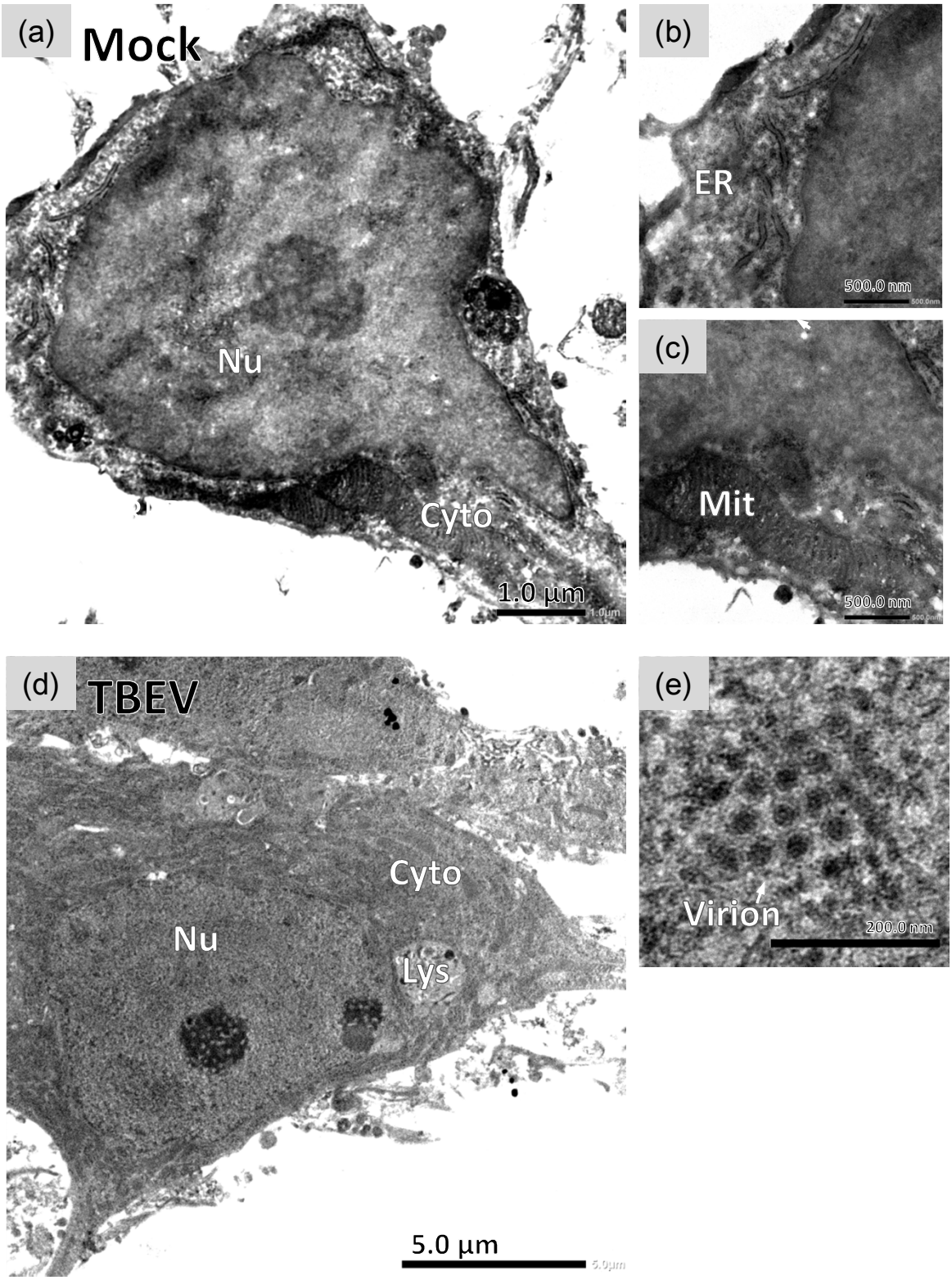
(a)
Mock
Nu
Cyto
1.0 µm
(b)
ER
500.0 nm
(c)
Mit
500.0 nm
(d)
TBEV
Cyto
Nu
Lys
5.0 µm
(e)
Virion
200.0 nm

Fig. 7 (2/2)

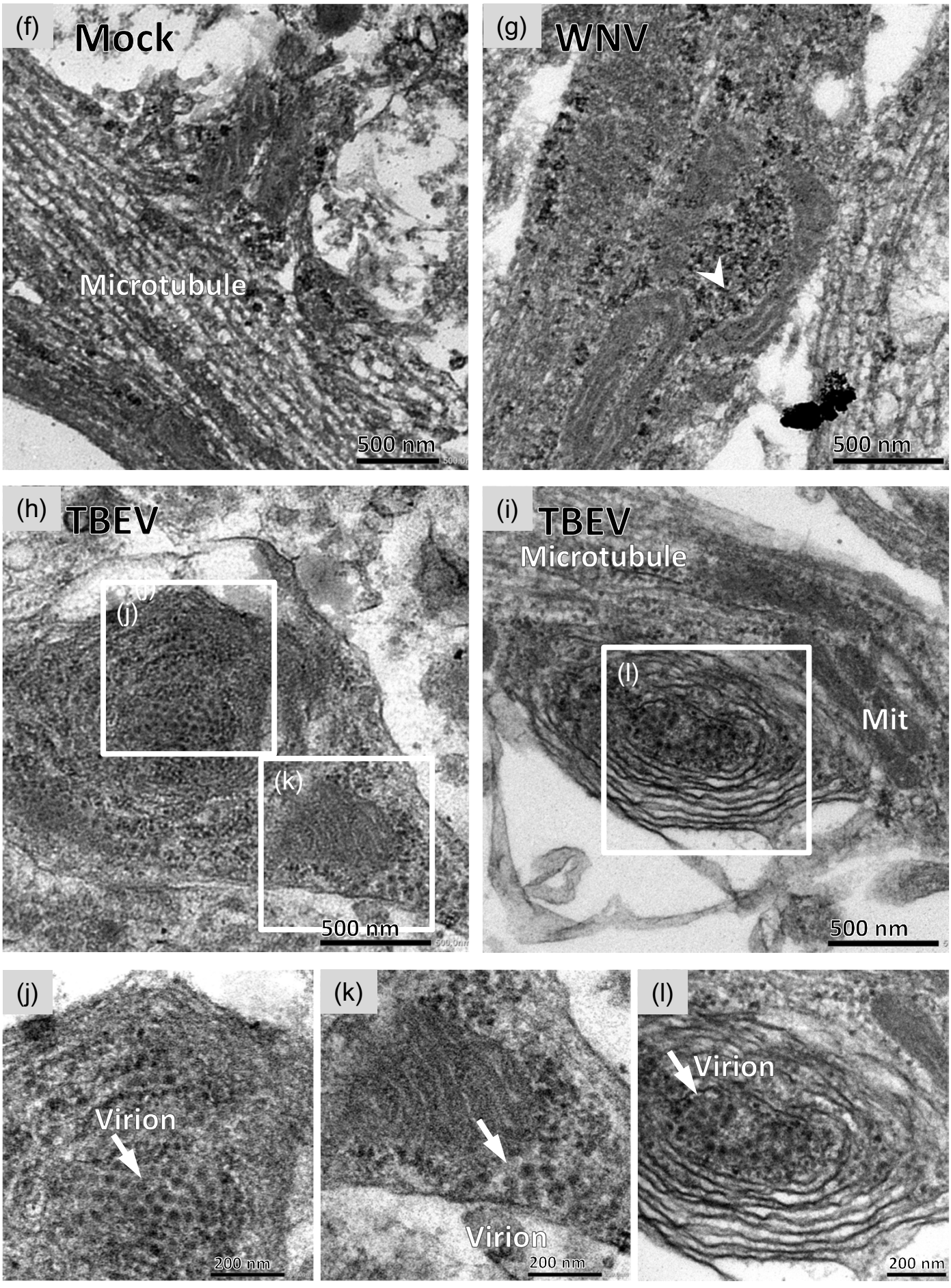
(f)
Mock
Microtubule
500 nm
(g)
WNV
500 nm
(h)
TBEV
(j)
(k)
500 nm
(i)
TBEV
Microtubule
(l)
Mit
500 nm
(j)
Virion
200 nm
(k)
Virion
200 nm
(l)
Virion
200 nm

Fig. 8

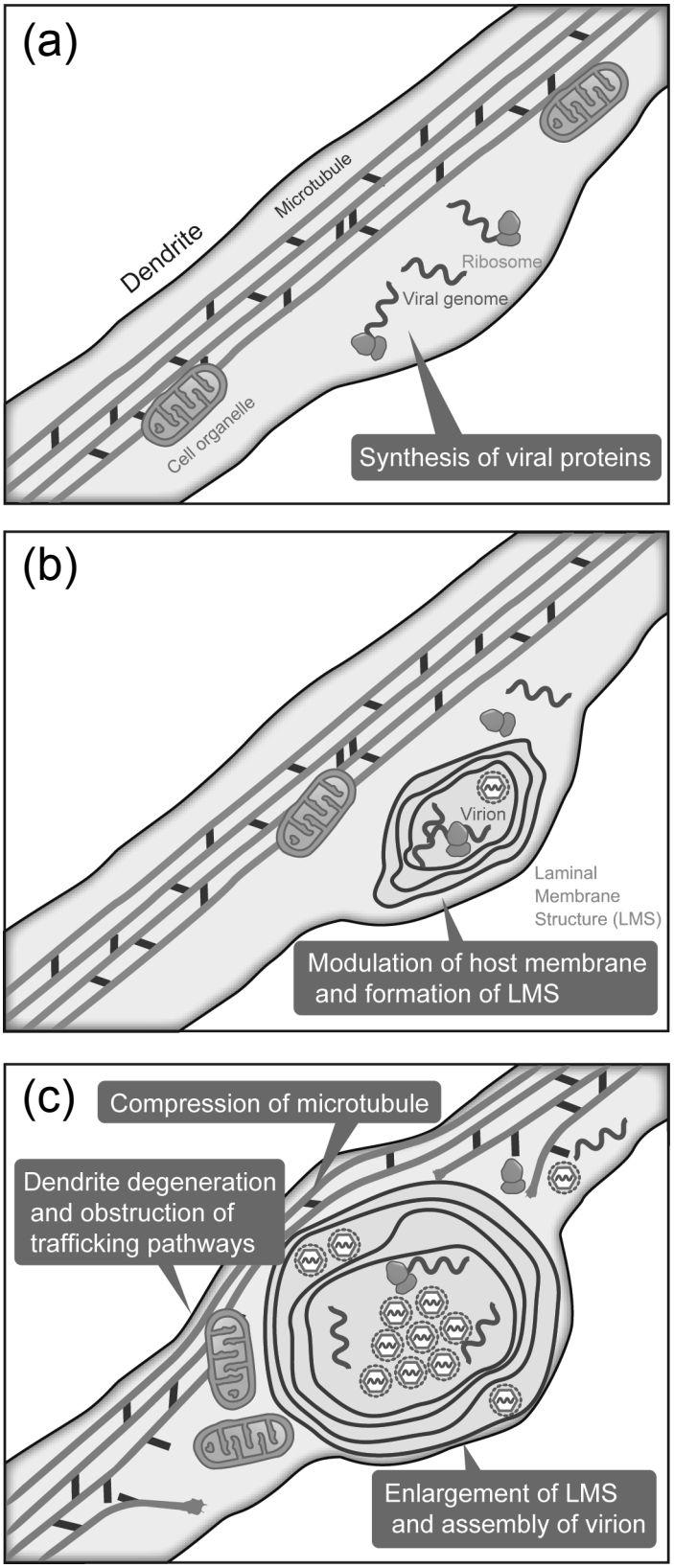
(a)
Dendrite
Microtubule
Ribosome
Viral genome
Cell organelle
Synthesis of viral proteins
(b)
Virion
Laminal
Membrane
Structure (LMS)
Modulation of host membrane
and formation of LMS
(c)
Compression of microtubule
Dendrite degeneration
and obstruction of
trafficking pathways
Enlargement of LMS
and assembly of virion